



## Effect of iron-manganese oxide on the degradation of deoxynivalenol in feed and enhancement of growth performance and intestinal health in weaned piglets

Caimei Wu<sup>a,1</sup>, Jingping Song<sup>a,1</sup>, Xinyue Liu<sup>b,1</sup>, Yuwei Zhang<sup>a</sup>, Ziyun Zhou<sup>a</sup>, David G. Thomas<sup>c</sup>, Bing Wu<sup>d</sup>, Xinru Yan<sup>d</sup>, Jian Li<sup>a</sup>, Ruinan Zhang<sup>a</sup>, Fali Wu<sup>a</sup>, Chuanmin Cheng<sup>e</sup>, Xiang Pu<sup>b</sup>, Xianxiang Wang<sup>b,\*</sup>

<sup>a</sup> Institute of Animal Nutrition, Sichuan Agricultural University, Key Laboratory for Animal Disease-Resistance Nutrition and Feedstuffs of China Ministry of Agriculture and Rural Affairs, Chengdu, Sichuan 611130, China

<sup>b</sup> College of Science, Sichuan Agricultural University, Chengdu, Sichuan 611130, China

<sup>c</sup> School of Agriculture and Environment, Massey University, Private Bag 11-222, Palmerston North 4442, New Zealand

<sup>d</sup> Chelota Biotechnology Co., Ltd., Guanghan, Deyang, Sichuan 618302, China

<sup>e</sup> Sichuan Provincial Feed Work Station, Chengdu, Sichuan 610041, China

### ARTICLE INFO

Edited by Dr. Caterina Faggio

#### Keywords:

Deoxynivalenol  
Iron-manganese oxide  
Detoxification  
Weaned piglets  
Growth performance

### ABSTRACT

Deoxynivalenol (DON), a prevalent and highly toxic mycotoxin in animal feed, poses significant risks to livestock health and productivity. This study evaluates the effectiveness of iron-manganese oxide (Fe/Mn oxides) in degrading DON. The DON degradation rate of Fe/Mn oxide reached 98.46 % in a controlled solution under specific conditions (0.2 % concentration, 37–85 °C, pH 6–7, 1-minute reaction time). When applied to actual feed, it reduced DON levels by approximately 49.3 % and remained stable in simulated gastrointestinal environments of weaned piglets. A 28-day trial involving 48 weaned piglets assessed the impacts of Fe/Mn oxides on health and growth. Results indicated that piglets consuming contaminated feed without the treatment exhibited reduced growth and compromised gut integrity, which were significantly mitigated by the addition of Fe/Mn oxides. Therefore, Fe/Mn oxides effectively reduce DON in feed and alleviate adverse health effects in piglets, making them a viable option to enhance safety and performance in mycotoxin-prone environments.

### 1. Introduction

Deoxynivalenol (DON), a secondary metabolite primarily synthesized by *Fusarium graminearum*, is recognized globally as one of the most prevalent and toxic field mycotoxins (Pestka and Smolinski, 2005). Research indicates a high detection rate of DON at 64 %, with notably elevated levels in Europe and Asia. Economically, DON contamination results in significant annual losses, estimated at several billion U.S. dollars worldwide, due to compromised crop quality (Anater et al., 2016). Pigs are particularly vulnerable to DON, which manifests in reduced feed intake, increased oxidative stress, and compromised intestinal barrier functions, consequently impairing their growth performance. The intestinal mucosa, including critical regions like the jejunum and ileum, suffers notably from DON exposure. Serving as the primary

defense against external pollutants, the intestinal mucosa consists of physical, chemical, immune, and microbial barriers. DON interferes with these protective mechanisms, first by damaging the physical barrier through alterations in the morphology and integrity of the intestinal epithelium. Additionally, it modifies the monosaccharide composition and expression of mucin, undermining mucosal protection, and compromises the immune barrier of the intestinal mucosa. Furthermore, alterations in the gut microbiome of pigs have been closely associated with DON ingestion. Hence, pigs consuming DON-contaminated feed typically exhibit symptoms such as growth retardation, weight loss, and anorexia (Dersjant-Li et al., 2007).

Reducing levels of DON in contaminated grains is pivotal for global agricultural health. Detoxification strategies include physical, chemical, and biological methods. While physical adsorption is widely used, it

\* Corresponding author.

E-mail address: [xianxiangwang@hotmail.com](mailto:xianxiangwang@hotmail.com) (X. Wang).

<sup>1</sup> Caimei Wu, Jingping Song and Xinyue Liu contributed equally to this work

often requires high temperatures or stringent conditions that increase feed production costs (Avantaggiato et al., 2004; Vila-Donat et al., 2018). Additionally, its lack of selectivity may compromise the nutritional quality of feed and lead to secondary pollution. Conversely, biological methods leverage the diverse activities of digestive enzymes and gut microorganisms but grapple with issues like unstable bonds between DON and absorbents. This instability can lead to localized spikes in DON levels, posing further health risks to livestock and poultry. Moreover, microbial and enzymatic interactions could reduce nutrient availability and produce harmful byproducts, diminishing the efficacy of these methods (Ji et al., 2016). The chemical detoxification approach is straightforward, cost-effective, and does not alter feed palatability. Moreover, the resulting chemical degradation products are highly stable, positioning chemical methods as likely candidates for extensive commercialization in the feed industry. Chemical detoxification of DON typically requires the establishment of extreme conditions, including acidic or alkaline treatments and oxidation or reduction processes. These methods, while effective at breaking down DON's chemical structure into less toxic products, can adversely affect the flavor and texture of feedstuff. As a result, such chemical processes are often coupled with physical detoxification techniques. Initially, milder physical methods like adsorption, selection, and soaking are employed to separate DON from the food matrix, followed by more aggressive chemical degradation. Oxidizing agents, such as ozone, are particularly effective at altering DON's structure through oxidation. Research indicates that DON is less stable under alkaline conditions than acidic ones, making it more susceptible to conversion into non-toxic or low-toxicity products (Schwartz et al., 2013). For example, extracting DON from noodles into a boiling solution and treating it with a 0.1 M  $\text{Na}_2\text{CO}_3$  (pH 11) solution can reduce the DON content in food samples by up to 93 %, effectively preventing its reintroduction into the environment (Ragab et al., 2009). Additionally, studies by Schwartz et al., (Schwartz et al., 2013) explored how different pH levels affect the degradation of DON using sodium bisulfite ( $\text{NaHSO}_3$ ) and sodium metabisulfite ( $\text{Na}_2\text{S}_2\text{O}_5$ ). Their findings indicate that DON can form three distinct sulfonates depending on the pH, with degradation products showing independence from the reagents employed. Remarkably, a sulfonate formed under acidic conditions could transform into two other types under alkaline conditions, underscoring the critical role of pH in the chemical degradation of DON and demonstrating that degradation primarily depends on the compound's alkalinity or oxidation level.

Metal oxides are well-known for their selective catalytic activity, allowing them to target and degrade specific substances under controlled conditions. For instance,  $\text{Fe}_3\text{O}_4$  anchored in porous charcoal successfully removes antibiotics from water (Peng et al., 2023b), and Co-doped  $\text{MnO}_2$  efficiently eliminates organic contaminants (Wang et al., 2023). The efficacy of these metal oxides is largely attributed to their ability to generate reactive oxygen species which catalyze oxidation processes to break down target molecules. In the field of animal nutrition, it is a common practice to supplement animal feed with trace nutritional elements, including iron and manganese salts (Palanisamy et al., 2023). Iron-manganese oxides (Fe/Mn dioxides) exhibit catalytic properties that facilitate the breakdown of large molecules, including DON, a prominent contaminant in this study. Fe-Co oxide nanocomposites have demonstrated the ability to efficiently remove aflatoxin B1 (AFB1) from edible oils through surface complexation and electrostatic interactions, exhibiting both efficacy and safety (Abasi et al., 2023). Additionally, manganese oxide is effective in degrading various mycotoxins, including DON in animal feed. Manganese ions possess a high redox potential, enabling the destruction of DON and its degradation into non-toxic and low-toxicity oxide (Su et al., 2024).

In this study, we aim to provide theoretical support for the widespread application of a novel DON chemical detoxification agent (DA) in animal production by investigating its detoxification efficacy and its effects on the intestinal health of weaned piglets. Our findings demonstrate that a porous compound containing iron and manganese can

effectively degrade DON by disrupting its toxic epoxy structures, thereby neutralizing the contaminant. Beyond its detoxification properties, this compound functions as a nutritional additive that enhances DON metabolism in the digestive systems of weaned piglets consuming contaminated feed. This dual functionality not only improves the intestinal health of the piglets but also promotes their overall growth. Additionally, we have shown that DA facilitates rapid detoxification during feed processing, effectively mitigating the adverse effects of DON on the intestinal health of weaned piglets, improving growth performance, reducing breeding costs, and promoting the sustainable use of crops. The strategic application of this detoxifying agent provides a theoretical foundation for the detoxification of bulk feed materials contaminated with DON, supports healthy livestock breeding, minimizes economic losses, and enables the rational utilization of moldy feed.

## 2. Materials and methods

### 2.1. Materials and instruments

DON standard product is purchased from Shanghai Yuanye Biotechnology Co., LTD., the specification is 5 mg/ branch, purity  $\geq 98$  %; Toxicogenic corn was fermented by our research group, and Fusarium gramineis, which was confirmed as DON toxigenic mould provided by the Plant protection Department of Sichuan Agricultural University, was utilized, the strain number was 15AC-20-7-11; Antioxidant Enzyme Activity Kit (Nanjing Jiancheng Biotechnology Co., LTD., Nanjing, China); Jiangsu Meimian ELISA kit (Jiangsu Meimian Industrial Co., Ltd, Yancheng, China); TruSeq™ DNA Sample PrepKit; HiscriPt-RIII RT kit; ChamQ Universal SYBR qPCR Master Mix kit; MJ-feces DNA extraction kit. Scanning Electron Microscopy (SEM) (Zeiss, Gemini300, Germany); X-Ray Diffraction (XRD) (Bruker AXS D8); X-Ray Photoelectron Spectroscopy (XPS) (Thermo Scientific, ESCALAB 250, Japan); Ultra-high Performance Liquid Chromatograph (UPLC, H-Class, waters, USA); High Performance Liquid Chromatography and Mass Spectrometry (HPLC-MS/MS, Agilent 1290Triple Quad, USA); QTOF (Agilent 6550, USA); Electronic Balance (ME204, METTLER TOLEDO); Automatic biochemical analyzer for Serum biochemical Indexes (7020, Hitachi Ltd., Tokyo, Japan); Microtome (Histo Core MULTICUT); Gas Chromatograph (CP-3800, VARIAN, USA). All reagents were analytically pure except some chromatographically pure reagents used in precision instruments.

### 2.2. Characterization of Fe/Mn dioxides and degradation products of DON

Fe/Mn dioxides, synthesized by Chelota Biotechnology Co., Ltd. in China as a chemical detoxification agent (DA), were analyzed. The morphology and size of the dioxides were examined using Scanning Electron Microscopy (SEM). Their structural properties were assessed with X-Ray Diffraction (XRD), while the elemental composition and valence state distribution were determined through X-Ray Photoelectron Spectroscopy (XPS). The interaction between the synthesized DA and the DON was explored using a liquid chromatography-mass spectrometry system (LCMS/MS and QTOF). The LCMS/MS employed a mobile phase consisting of a 0.1 % formic acid aqueous solution mixed with acetonitrile in various proportions, optimized for the most effective separation. The analytical column used was a Waters BEH C18 (2.1  $\times$  100 mm, 1.7  $\mu\text{m}$  particle size), with a flow rate set at 0.3 mL/min and an injection volume of 5  $\mu\text{L}$ . A detailed analysis of the LCMS/MS data provided insights into the potential degradation pathways and mechanisms of DON catalyzed by DA.

### 2.3. Degradation of DON in vitro

DON standards were prepared in acetonitrile water (1:9) at

concentrations of 1.5 mg/L and 3.0 mg/L (Garai et al., 2021), the pH value of a 0.2 % aqueous solution of DA is 4.26. A single-factor experiment was conducted to optimize the dosage, pH, time, and temperature for the detoxification agent (DA) to degrade DON. To simulate the extracorporeal gastrointestinal environment of pigs, artificial gastric and intestinal fluids were prepared. The gastric fluid was composed of 0.3 g/L pepsin, 13.1 g/L NaCl, 1.1 g/L KCl, 0.15 g/L CaCl<sub>2</sub>, and 0.6 g/L NaHCO<sub>3</sub>, with the pH adjusted to 2.7 using 1 mol/L HCl. The intestinal fluid was adjusted from the gastric fluid to a pH of 7.2–7.6 using 1 mol/L NaOH, with additions of 4.5 g trypsin and 45 mg bile salts. During the production of piglet compound feed, varying concentrations of DA were incorporated. This process was conducted at temperatures ranging from 65 to 85 °C, with a feed pH of 5.85 and 20 % moisture content, to study the decontamination of feed raw materials and evaluate the efficiency of DA in degrading DON within the feed. Post-decontamination, the feed was mixed with the simulated gastric and intestinal fluids and subjected to an oscillating reaction at 37 °C for 2 h. The supernatant was then sampled to assess the DON concentration, aiming to explore the dissociation behavior of DON post-detoxification in a simulated porcine gastrointestinal system.

The extraction of DON from feed was carried out according to GB/T30956–2014 method, and the detection of DON was determined by HPLC-MS/MS method. The degradation rate,  $Q_1$ , was calculated using formula (1):  $D_1 = (C_0 - C_1)/C_0 \times 100\%$ , where ( $C_0$ ) is the initial DON concentration, and ( $C_1$ ) is the concentration in the supernatant post-degradation. The dissociation rate,  $D_2$ , was calculated using formula (2):  $D_2 = (M_1 - M_2)/M_0 \times 100\%$ . In this formula, ( $M_1$ ) denotes the content of DON in the supernatant after mixing the degraded feed with artificial gastric and intestinal fluids, ( $M_2$ ) represents the DON content in feed raw materials post-degradation, and ( $M_0$ ) is the initial DON content in the feed raw materials before any treatment.

#### 2.4. Experimental animals, diets, and design

The Animal Care and Use Committee of Sichuan Agricultural University (Chengdu, China, approval code: 20220230) sanctioned all experimental procedures. Forty-eight weaned piglets of the Duroc×Landrace×Yorkshire breed, averaging  $7.57 \pm 0.40$  kg in body weight and  $25 \pm 1$  days old, were randomly assigned to one of four dietary treatments. Each treatment comprised six replicates, with each replicate containing two piglets. The groups included: a control group (CON) fed a basal diet; a DA group fed a basal diet supplemented with 0.2 % DA; a DON-contaminated group fed a basal diet with 3.55 mg/kg of DON; and a DON + DA group fed a DON-contaminated diet plus 0.2 % DA. Initial average body weights were statistically similar across all groups, and the sex ratio was evenly balanced at 1:1. Individual enclosures were provided for each piglet, ensuring free access to both feed and water. Disinfection and immunization protocols were aligned with the standard practices of the hosting pig farm. A preliminary feeding period of 7 days preceded the formal experimental phase, which extended over 28 days.

#### 2.5. Preparation of DON-contaminated corn and determination of dietary Mycotoxin content

The experimental diet adhered to the nutritional guidelines for weaned piglets as recommended by the NRC (2012) (Council USNR, 2012), utilizing a corn-soybean meal as the basal feed. The composition and nutrient levels of the basal diet are shown in the Table S1. The toxic corn was inoculated with mold spores, fermented for 25 days at 25 °C and 75 % moisture, and then sterilized (Tang et al., 2021). The corn was dried at 65 °C and crushed. When the moldy corn was added to the basal diet, the final concentration of DON in the combined diet of the DON group reached 3.55 mg/kg. The content of DON, aflatoxin B1 (AFB1), fumonisin B1 (FB1), T2 and zearalenone (ZEN) in diets were determined by HPLC-MS/MS method. The mycotoxin concentration of the feed and

the feed hygiene standard (GB13078–2017) are shown in the Table S2.

#### 2.6. Sample collection

Weight measurements for each piglet were made at both the start (day 0) and the conclusion (day 28) of the study, with feed consumption logged daily. At the end of the period, we calculated key metrics for each piglet, including average daily gain, average daily feed intake, and feed-to-gain ratio. On day 29, six pigs (comprising three boars and three sows) from each treatment group were randomly selected for the collection of blood samples. Blood was drawn from the external jugular vein and collected into coagulation accelerator tubes, followed by serum extraction via centrifugation at 1200 g and 4 °C for 15 minutes. Following the collection of blood, the pigs were euthanized using an intravenous injection of sodium pentobarbital, then dissected to segregate intestinal segments. From these segments, two consecutive cuts were made from the middle of the duodenum, jejunum, and ileum for both histological evaluations and mucosal collections. These approximately 2.0 cm intestinal segments were cleansed with cold PBS (Phosphate-buffered saline) and fixed in 4 % paraformaldehyde to aid in morphological assessments. Subsequently, the duodenum, jejunum, and ileum were slit lengthwise, washed with cold PBS, and the mucosal samples were carefully scraped with sterile glass microscope slides. These samples were instantly frozen in liquid nitrogen and preserved at –80 °C for future analysis. Lastly, cecal chyme was collected into sterilized containers and immediately frozen at –80 °C, to be later used in the analysis of intestinal microflora composition.

#### 2.7. Intestinal morphology

Sections of the duodenum, jejunum, and ileum were carefully removed from the 4 % paraformaldehyde fixative solution. A 2 mm thick cross-section was precisely cut with a blade and then placed into an embedding box, individually numbered. These sections were washed overnight under running water. Following this process, each sample underwent dehydration through a series of graded alcohol solutions prior to embedding in paraffin wax. Subsequently, 5 μm thick wax sections were prepared and stained using hematoxylin and eosin. The detailed morphology and structural arrangements of the duodenal, jejunal, and ileal tissues were examined and documented using the BX43 microscopic image workstation. Using the CapStudio-SC600C software, the villus height and crypt depth of each tissue from the selected fields of vision at 40x magnification were meticulously measured. The data collected facilitated the calculation of the ratio between villus height and crypt depth, providing key insights into the intestinal architecture of the piglets.

#### 2.8. Detection of cytokines, D-lactic acid and diamine oxidase (DAO) in serum

The activity of DAO and the concentration of D-lactic acid were determined using ELISA kit, according to the kit instructions. Similarly, Jiangsu Meimian ELISA kits were used to measure serum immune related indicators IgA, IgG, TNF-α, IL-6, IL-8, IL-1β, and concentration of INF-γ, according to the kit instructions.

#### 2.9. Expression of mRNA by real-time PCR

Total RNA was extracted from the duodenal, jejunal, and ileal tissue using Trizol reagent. The purity and concentration of total RNA were determined by an ultramicroscopic spectrophotometer (Nano Drop 2000/2000C). The ratio of A260/280 should be between 1.8 and 2.0. cDNA was reverse-transcribed using HiscriPt®III RT kit, synthesized and stored at –80 °C. Real-time fluorescence quantitative PCR was performed using a ChamQ Universal SYBR qPCR Master Mix kit. The RCR cycling conditions were as follows: 30 s at 95 °C, followed by 40 cycles

of 10 s at 95 °C and 30 s at 60 °C. Melt curve analysis was used to confirm specificity of the amplified product. The primer sequence is shown in Table S3. The  $\beta$ -actin was the internal genes. The  $2^{-\Delta\Delta CT}$  method was used to calculate mRNA expression level relatively.

### 2.10. Cecal microbial population analysis

The composition of microflora in cecal digesta was analyzed by 16 s rRNA sequencing. The genomic DNA of 24 cecal digesta samples was extracted using a MJ-feces DNA extraction kit. The extracted genomic DNA was detected by 1 % agarose gel electrophoresis after extraction. Specific primers with barcodes were synthesized for PCR amplification according to 16S V3 - V4 region corresponding to the primers. After PCR amplification, PCR products were quantified using the QuantiFluor™-ST Blue fluorescence quantification system (Promega). A Miseq library was constructed using TruSeq™ DNA Sample PrepKit reagent. Illumina's NovaSeq PE250 platform was used for sequencing. PE reads obtained by Miseq sequencing were spliced according to their overlap, and high-quality sequences were screened out. After samples were distinguished, microbial OTU cluster analysis, microbial species taxonomic analysis and various diversity index analysis could be carried out.

### 2.11. Statistical analysis

The data were analyzed using PROC MIXED in SAS 9.4 (SAS Institute Inc., Cary, NC, USA) and post hoc testing was conducted using Duncan's multiple comparison tests. The data are presented as means and pooled SEM. Differences were considered significant if  $P < 0.05$  and to reflect a tendency if  $0.05 \leq P < 0.10$ .

## 3. Results and discussion

### 3.1. Characterization of DA

The detoxification agent (DA), designed to target DON and incorporate iron and manganese oxides, was developed by Chelota Biotechnology Co., Ltd. in China. This process involved loading iron-based and manganese-based nanomaterials onto a sodium-based, water-soluble carrier. The appearance of DA is a white powder (Fig. 1A). Scanning electron microscopy (SEM) images of DA (Fig. 1B) showcase a porous morphology characterized by irregular shapes and numerous protruding sites on the surface, suggesting a structure with a large surface area optimal for the adsorption of active materials and provision of effective catalytic sites. Elemental mapping (Fig. 1G and H) reveals that DA is enriched with oxygen (O), carbon (C), iron (Fe), and manganese (Mn). X-ray diffraction (XRD) analysis (Fig. 1C) indicates that  $MnO_2$

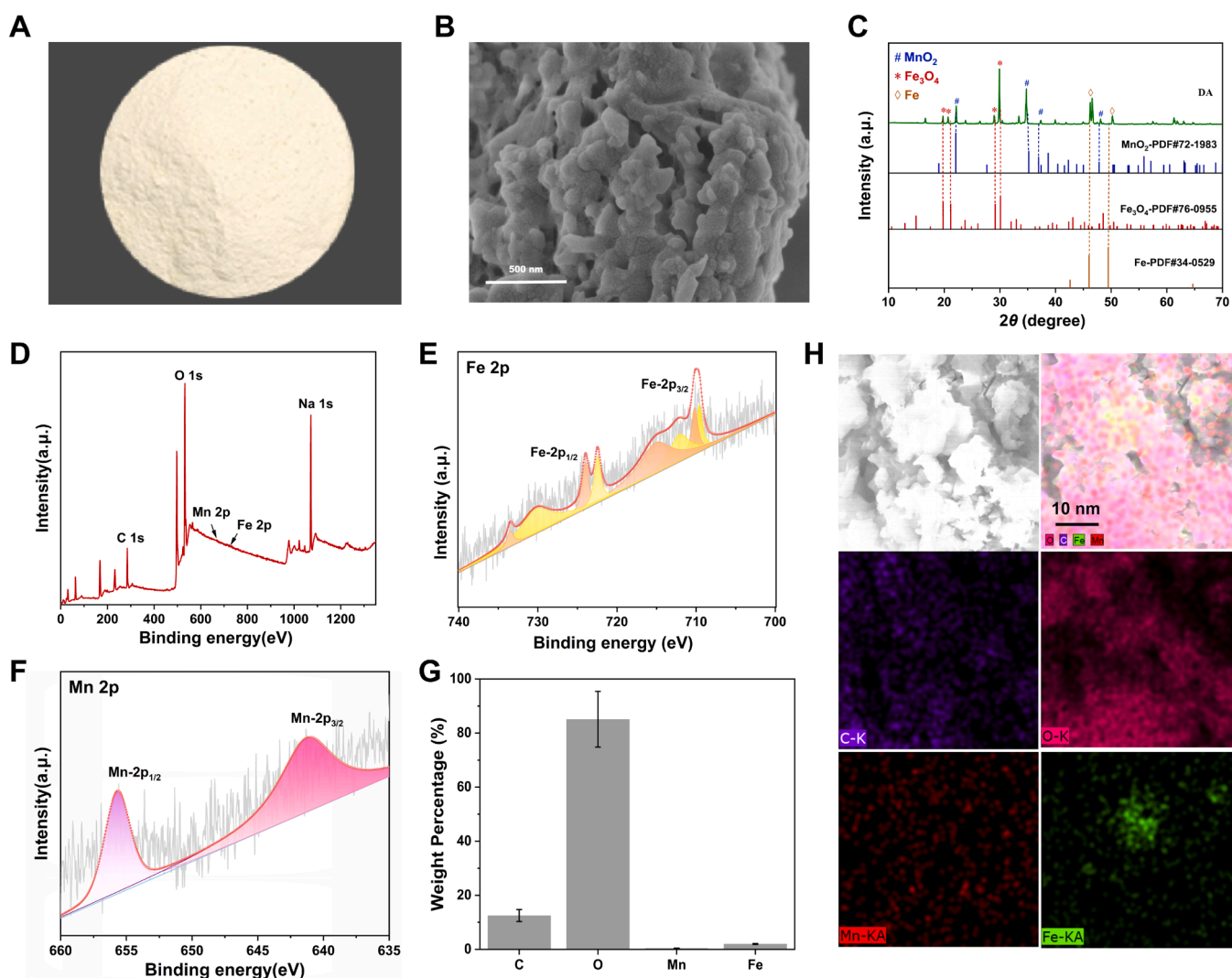


**Fig. 1.** Characterization of DA. (A) DON chemical detoxification agent, (B) SEM image of DA, (C) XRD pattern of DA, (D) Survey XPS spectra of DA, (E) Fe 2p, (F) Mn 2p XPS spectra of DA, (G) Image of element mass distribution of DA and (H) TEM mapping of the DA.



(PDF#72–1983),  $\text{Fe}_3\text{O}_4$  (PDF#76–0955), and Fe (PDF#34–0529) are the primary crystalline phases present in DA. The X-ray photoelectron spectroscopy (XPS) full spectrum (Fig. 1D) further corroborates these findings, highlighting O, Na, and C as the predominant elements, with the additional presence of Fe and Mn confirmed through mapping results. Detailed spectral analysis reveals peaks at 709.5 eV and 722.4 eV attributed to  $\text{Fe}^{2+}$  and its two satellite peaks at 712.1 eV and 730.1 eV; likewise, peaks at 710.4 eV and 724.0 eV correspond to  $\text{Fe}^{3+}$ , with satellite peaks at 715.1 eV and 733.5 eV respectively (Fig. 1E). The existence of  $\text{Mn}^{2+}$  is affirmed by spectral peaks at Mn 2p1/2 (655.7 eV) and Mn 2p3/2 (641.1 eV) (Fig. 1F).

### 3.2. Degradation of DON in vitro

We have optimized the reaction conditions for DA to effectively degrade DON. The optimal dosage of DA, as presented in Fig. 2A, is 0.2 %. At this concentration, the degradation rates for DON at 3 mg/L and 1.5 mg/L reached 96.76 % and 95.94 %, respectively, significantly outperforming other concentrations tested. The acidic nature of the DA solution may account for the lower effectiveness at higher concentrations. Further analysis indicates the optimal pH for this reaction; as displayed in Fig. 2B, pH levels 6.2, 7.2, and 8.3 showed degradation rates of 96.10 %, 98.46 %, and 98.13 % respectively, with no significant differences among these outcomes. Considering the typical pH of feed is around 6, we established the optimal reaction pH for DA degradation of DON at 6.2. Temperature effects on degradation rates, as depicted in Fig. 2C, were significant only at higher temperatures. Observing substantial degradation at both 65 °C and 85 °C allowed us to choose the more energy-efficient 65 °C as the optimal temperature. Reaction time, as shown in Fig. 2D, minimally affected degradation rates, leading us to select a duration of 1 min for practical application. Based on these findings, the optimal parameters for degrading DON using DA are a dosage of 0.2 %, a system pH of 6.2, a detoxification temperature of 65

°C, and a detoxification duration of 1 minute. Under these conditions, a maximum degradation rate of 98.46 % was achieved.

To ascertain the optimal DA concentration for detoxifying feed intended for weaned piglets, we tested DA levels from 0.1 % to 1.0 %. As illustrated in Fig. 2E, concentrations below 0.2 % yielded a degradation rate of 49.28 %, which was superior to other concentrations tested; thus, 0.2 % was selected. Notably, the degradation rate of DON in standard solutions was higher than that in processed feed, potentially due to feed components interfering with the DA - DON reaction. The robust redox properties of DA likely facilitate the disruption of the cyclic oxygen structure at  $\text{C}_{12}$  -  $\text{C}_{13}$  in the DON molecule, enhancing toxin degradation. We assessed the potential for dissociation post-DA detoxification of DON by simulating the porcine gastric and intestinal environments, with results displayed in Fig. 2F showing dissociation rates in simulated gastric fluid of 2.99 %, 4.73 %, 7.27 %, and 3.32 %. These figures suggest slight dissociation in the stomach, potentially due to incomplete reactions in the feed at pH 6.2. Upon transition to artificial gastric fluid at pH 2.7, increased contact area and moisture content, along with the inherently acidic DA solution, may have contributed to some dissociation, although the overall dissociation rate remained below 10 %. As the dissociated liquid transitioned to the pig's small intestine, where pH levels rise, DON underwent further degradation, culminating in final dissociation rates below 1 %. Thus, only a minor portion of DON dissociated in the gastrointestinal tract post-detoxification, affirming that DA can effectively and stably degrade DON in feed. The conditions required for employing DA in DON degradation are easily met during the feed production process, endorsing DA's suitability for detoxifying feed.

### 3.3. Degradation mechanism of DON by DA

Utilizing liquid chromatography-mass spectrometry, we further explored the degradation mechanism of DON by DA. The results from mass spectrometry are presented in Error! Reference source not found.

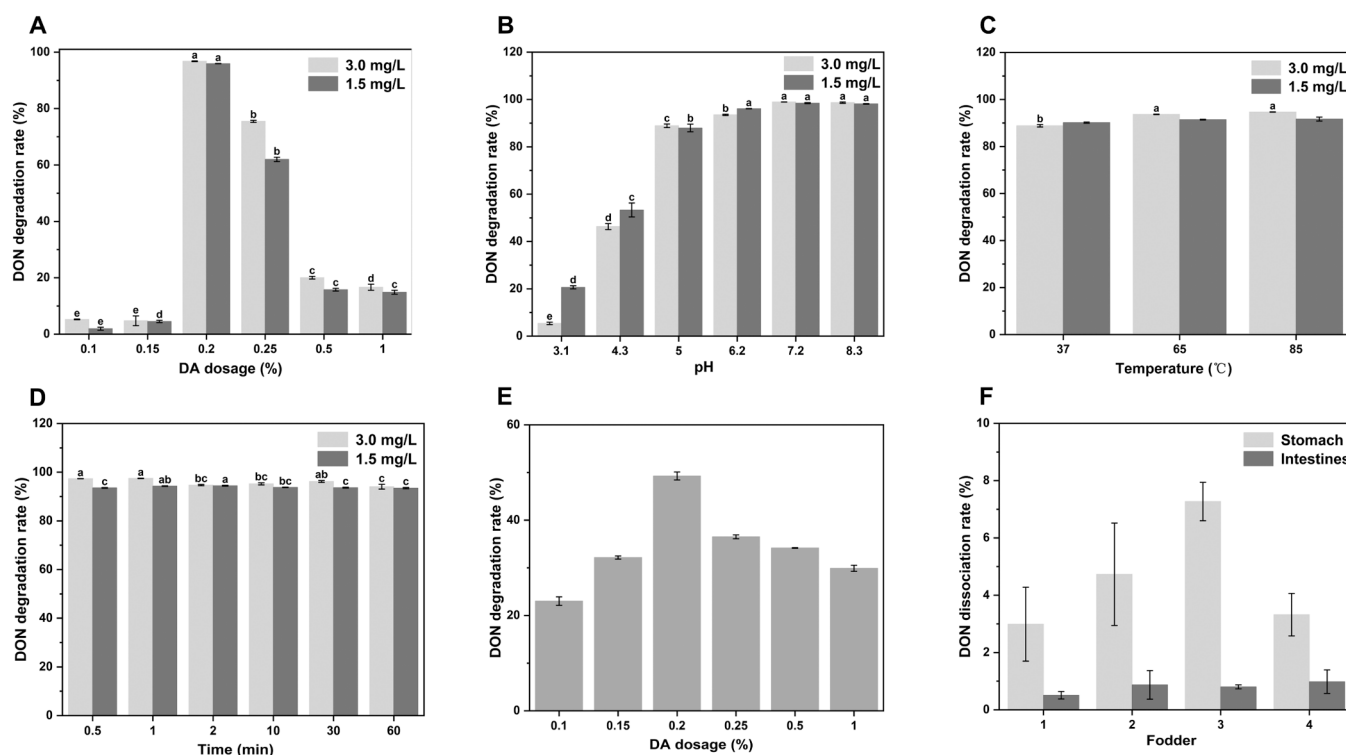


Fig. 2. DA degradation of DON *in vitro* under optimal reaction conditions, degradation rate and simulated dissociation of small intestinal fluid. (A) The optimal reaction dose, (B) pH, (C) temperature and (D) time of DA to degrade DON, (E) The detoxification effectiveness of DA in degrading DON in feed and (F) the dissociation of DON degraded by DA in a simulated gastrointestinal environment of pigs. Data are mean  $\pm$  SE ( $n = 3$ ). Data labelled with different low-case letters are statistically different at  $p < 0.01$ .

DON, a mono-terminal sporene, is subjected to oxidative degradation by DA, a porous material with a core of MnO<sub>2</sub> and Fe<sub>3</sub>O<sub>4</sub> (Peng et al., 2023a). This treatment initially targets the unsaturated carbon-carbon double bonds at positions C<sub>9</sub> and C<sub>10</sub>, transforming them into an open-ring aldehyde/ketone structure labeled as Product 1 ([M + H]<sup>+</sup>: *m/z* 329.1593). This is followed by the deoxygenation of the epoxy groups, while the hydroxyl group at position C<sub>7</sub> undergoes oxidative dehydrogenation, generating Product 2 ([M + H]<sup>+</sup>: *m/z* 311.1273). The aldehyde group in Product 2 is further oxidized to a carboxylic group by DA, resulting in Product 3 ([M + H]<sup>+</sup>: *m/z* 327.2014). Similarly, the unsaturated bonds at positions C<sub>12</sub> and C<sub>13</sub>, along with the  $\alpha$ -methyl group at C<sub>9</sub>, are oxidized to form Product 4 ([M + H]<sup>+</sup>: *m/z* 331.1046). Subsequent oxidation by DA opens and oxidizes the cyclopentanone ring to produce Product 5, where further oxidation of the aldehyde group results in Product 6 ([M + H]<sup>+</sup>: *m/z* 347.7528). The middle ring then undergoes oxidation and opening, leading to intermediate 7 ([M + H]<sup>+</sup>: *m/z* 348.2583). Its aldehyde group is transformed into a carboxylic group, culminating in the formation of the tetracarboxylic acid form as Product 8 ([M + H]<sup>+</sup>: *m/z* 362.3293). Due to the molecular instability of adjacent carbonyl groups, a continuous carbonyl elimination process occurs under DA's influence, generating a series of tetracarboxylic acid products, Products 9–11. Additionally, the presence of the CN anion from the acetonitrile solvent triggers nucleophilic additions to the aldehyde groups of Product 1 and Product 2, generating Product 12 ([M + H]<sup>+</sup>: *m/z* 356.2010) and Product 13 ([M + H]<sup>+</sup>: *m/z* 338.3485). These oxidation products, marked in blue, are notably prevalent in the reaction mixture (Liu et al., 2023a). These results demonstrate that DA primarily facilitates DON degradation by oxidizing the unsaturated carbon-carbon double bonds at C<sub>9</sub> and C<sub>10</sub>, as well as the epoxy groups at C<sub>12</sub> and C<sub>13</sub>. Throughout the process, the cyclopentanone and tetrahydropyran rings are converted into binary, tertiary, and quaternary carboxylic acids, enhancing the degradative and detoxifying effects. Complementary research has shown that redox-reactive chemical materials such as CuO-Cu<sub>2</sub>O/WO<sub>3</sub> ternary thin films can efficiently degrade DON (Cheng et al., 2021). The potent oxidative capacity of active radicals prompts the cleavage of -OH groups on the DON ring, while the unstable toxic epoxy structures at C<sub>12</sub> and C<sub>13</sub>, susceptible to attack by O<sup>2-</sup>, convert into carbonyl groups, ultimately transforming into carboxylic acids.

### 3.4. Effects of DA on growth performance of weaned piglets

Compared to ruminants and poultry, pigs are more vulnerable to DON due to their reduced capacity for detoxification. Studies have shown that chronic exposure to low doses of DON can decrease pigs feed intake, daily weight gain, and nutrient absorption efficiency. The results of this study, as depicted in Table 1, indicate no significant differences in the initial body weight among all treatment groups of weaned piglets ( $P > 0.05$ ). However, relative to the control (CON) group, the presence of DON notably reduced final body weight, average daily gain (ADG), and average daily feed intake (ADFI) ( $P < 0.01$ ). In contrast, compared to the DON group, the addition of DA significantly increased average daily feed intake (ADFI) ( $P < 0.01$ ), although it had no significant impact on final body weight and ADG ( $P > 0.05$ ). Furthermore, DON is known to inhibit feed intake and may provoke vomiting, thereby adversely affecting growth performance. In this experiment, exposure to DON resulted in a 26 % reduction in the ADG of weaned piglets, aligning with findings from previous research. The ADG of weaned piglets increased by 11 % when DA was added to the DON diet. There was no significant difference in F/G in the DON group compared with the CON group, proving that the DON toxin had limited or no effect on F/G. The result suggested that the decreased growth performance may be mainly due to reduced feed intake rather than reduced nutrient utilization. Since there was no difference in F/G in the DON group, it is possible that intestinal damage caused by DON becomes less severe over time (Lafleur Lariviere et al., 2021). Commonly, a reduction in average daily feed intake (ADFI) is the most evident effect of DON exposure in pigs. In this study, DON exposure

**Table 1**

The performance of weaned piglets on the four dietary treatments.

Items	Treatment				SEM	P-value
	CON <sup>1</sup>	DA <sup>2</sup>	DON <sup>3</sup>	DON+DA <sup>4</sup>		
Initial body weight, kg	7.43	7.49	7.66	7.70	0.128	0.389
Final body weight, kg	16.79 <sup>a</sup>	17.61 <sup>a</sup>	14.55 <sup>b</sup>	15.47 <sup>b</sup>	0.377	<0.01
Average daily feed intake, g/d	506.35 <sup>b</sup>	543.07 <sup>a</sup>	369.63 <sup>d</sup>	427.98 <sup>c</sup>	10.473	<0.01
Average daily gain, g/d	334.38 <sup>a</sup>	361.61 <sup>a</sup>	245.98 <sup>b</sup>	277.53 <sup>b</sup>	12.489	<0.01
Ratio (feed/gain)	1.52	1.51	1.54	1.57	0.050	0.850

<sup>1</sup>The control group (CON), weaned piglets fed with a basal diet; <sup>2</sup>The DA group (DA), weaned piglets fed with a basal diet + 0.2 %DA; <sup>3</sup>DON group (DON), weaned piglets fed with a basal diet containing 3.55 mg/kg DON; <sup>4</sup>DON + DA group (DON + DA), weaned piglets fed with a basal diet containing 3.55 mg/kg DON + 0.2 % DA. Data are mean  $\pm$  SE (n = 6). <sup>a, b, c</sup> Different letters in the same row indicate significant differences ( $p < 0.05$ ), no letters in the same line or the same letters in the data shoulder indicate that the difference is not significant ( $p > 0.05$ ).

resulted in a 27 % decrease in ADFI among weaned piglets, closely mirroring the 26 % reduction reported by Andretta et al. in a meta-analysis (Andretta et al., 2012). Moreover, adding DA to the DON diet led to a 14 % increase in ADFI.

### 3.5. Effects of DA on intestinal morphology and permeability in weaned piglets

DON, a mycotoxin, negatively affects the intestinal mucosa's morphology and function, which are vital indicators of gut health. It causes histological alterations including villi atrophy, fusion of villi, necrosis of apical villi, and diminished villi height. This research aimed to evaluate the impact of DON on key morphological features including villus height, crypt depth, and the villus height to crypt depth ratio across different sections of the intestine (duodenum, jejunum, and ileum) in weaned piglets. Additionally, the study investigated the potential mitigative effects of DA on these parameters. As indicated in Table S4 and Fig. 3A, compared to the control (CON) group, DON significantly reduced villus height and the villus height/crypt depth ratio, and increased crypt depth in all tested intestinal sections ( $P < 0.05$ ). In contrast, DA treatment resulted in a significant increase in villus height and villus height/crypt depth ratio, and a decrease in crypt depth in the jejunum, when compared to the DON group ( $P < 0.05$ ). Previous research supports these findings, showing that a diet containing 2.8 mg/kg DON fed to 10 kg weaned piglets over 35 d notably decreased villus height in the jejunum and increased lesion formation in the jejunum and ileum. These studies underline that DON significantly lowers villus height and increases crypt depth, negatively impacting nutrient absorption and utilization in the small intestine. The findings of this experiment align with prior research, revealing that exposure to DON substantially decreases villus height and villus height/crypt depth ratio, and increases crypt depth. However, incorporating DA into the DON-contaminated diet notably improved these intestinal morphological indices in weaned piglets, enhancing villus height and reducing crypt depth.

Diamine oxidase (DAO) content and activity serve as effective indicators of intestinal permeability in mammals. Typically, DAO levels are elevated in the villi of the small intestine while being less pronounced in other tissues. Damage to the intestinal mucosa allows DAO to enter the bloodstream, leading to increased DAO activity in plasma. Lactic acid, primarily produced by bacterial fermentation, is generally not rapidly absorbed or degraded in mammals. Consequently,

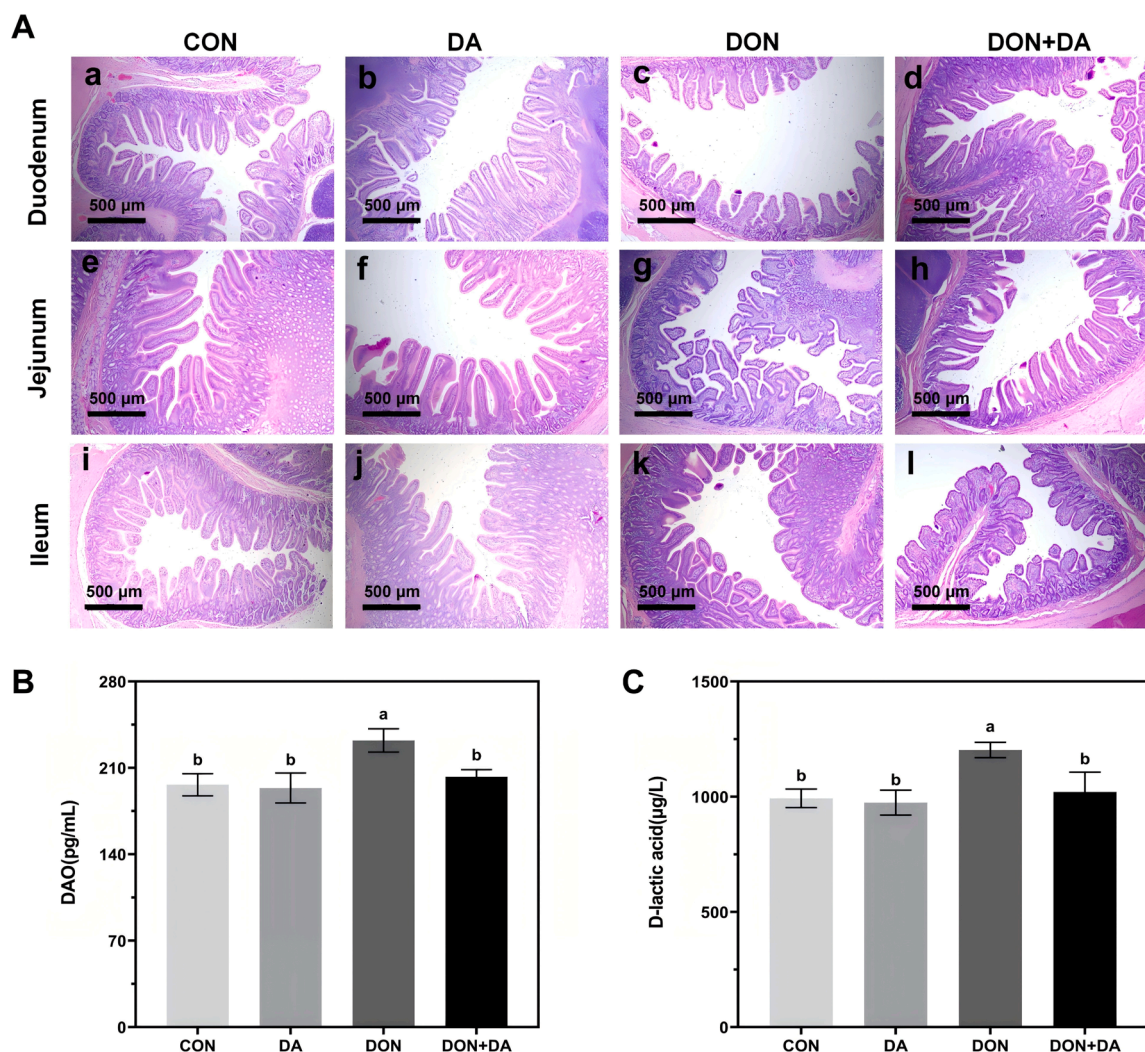


**Fig. 3.** Effects of DA on the intestinal morphology and permeability indicators of weaned piglets. (A) Effects of DA on the duodenum, jejunum and ileum morphology of weaned piglets (40 $\times$ ), (B, C) Effects of DA on the intestinal permeability indicators of weaned piglets. Data are mean  $\pm$  SE (n = 6). Data labelled with different low-case letters are statistically different at  $p < 0.05$ .

augmented intestinal permeability permits D-lactic acid from intestinal bacteria to infiltrate the bloodstream via compromised mucosal tissues. Therefore, plasma levels of DAO and D-lactic acid often signify the degree of damage to the intestinal barrier, commonly referred to as intestinal permeability.

The impact of deoxynivalenol (DON) and diamine (DA) on intestinal permeability indicators in weaned piglets is illustrated in Fig. 3B and C. Compared to the control group (CON), DON markedly elevated serum diamine oxidase (DAO) and D-lactic acid levels ( $P < 0.05$ ). Conversely, DA administration significantly lowered these serum concentrations compared to the DON group ( $P < 0.05$ ). This study observed that serum DAO and D-lactic acid concentrations increased in weaned piglets fed a DON-contaminated diet, suggesting damage to the intestinal mucosa. This finding aligns with previously published research. Moreover, DA was effective in reducing serum levels of DAO and D-lactic acid, indicating that it can mitigate intestinal mucosal damage induced by DON in piglet diets. The results further revealed that DON disrupts the intestinal physical barrier by altering intestinal morphology and permeability. In contrast, DA appears to protect against these effects by degrading DON in vitro, which reduces its detrimental impact on intestinal morphology and permeability, thereby preserving the physical barrier integrity of the piglets' intestines.

### 3.6. Expression levels of physical barrier related genes

Tight junctions (TJs) are crucial in maintaining intestinal health as they are involved in the formation and development of the intestinal epithelium, maintenance of epithelial integrity, and regulation of permeability. DON can influence the expression of TJ proteins in animals. Fig. 4A–C depict the effects of a DA on the mRNA expression levels of genes associated with the physical barrier in the duodenum, jejunum, and ileum of weaned piglets. Relative to the control group (CON), DON significantly diminished the mRNA levels of *claudin-3* in the duodenum ( $P < 0.05$ ). However, DA did not significantly impact the mRNA levels of genes related to the physical barrier in the jejunum and ileum ( $P > 0.05$ ).

Ling et al. found that DON up-regulated mRNA expression of *claudin-1*, *claudin-4*, *occludin* and *ZO-1*, but down-regulated mRNA expression of *claudin-3* (Ling et al., 2016). Studies have shown that in response to chronic and long-term DON exposure, occludin protein expression in intestine of piglets is down-regulated. In another study, mRNA expression levels of *claudin-4* and *occludin* were up-regulated in the jejunum after a low dose (0.9 mg/kg) and short-term (10 days) exposure to DON in growing pigs, with mRNA expression levels of *claudin-1*, *claudin-3*, *claudin-4* and *occludin* down-regulated in the ileum, cecum and colon (Alizadeh et al., 2015). This suggests that short term, low dose exposure to DON can also cause changes in intestinal TJ of piglets.



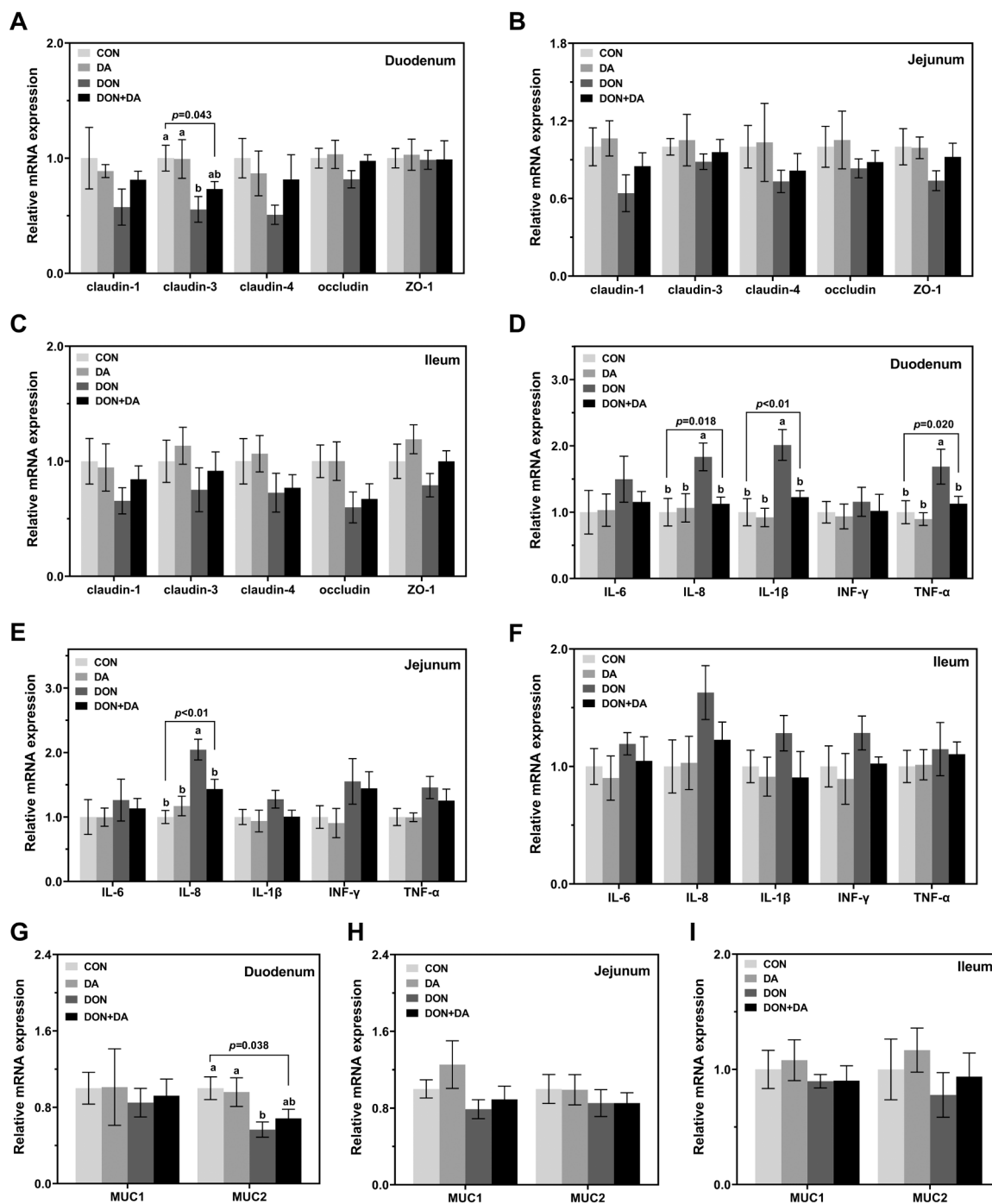


**Fig. 4.** Effects of DA on the intestinal physics, chemistry and immune barrier function of weaned piglets. (A, B, C) Effects of DA on the relative mRNA levels of tight junction proteins in the duodenum (A), jejunum (B) and ileum (C) of weaned piglets, (D, E, F) Effects of DA on the relative mRNA levels of pro-inflammatory factor in the duodenum (D), jejunum (E) and ileum (F) of weaned piglets, (G, H, I) Effects of DA on the relative mRNA levels of mucin in the duodenum (G), jejunum (H) and ileum (I) of weaned piglets. Data are mean  $\pm$  SE ( $n = 6$ ). Data labelled with different low-case letters are statistically different at  $p < 0.05$ .

It is worth noting, in contrast to the results of previous studies, this study found that DON had no significant effect on the expression of TJ-related genes in the jejunum and ileum of weaned piglets, and the difference in results may be related to the dose and exposure time of DON. In addition, pig intestinal epithelium is completely renewed every two to three days (Verdile et al., 2019), a property that may also interfere with mRNA expression. The intestinal epithelial TJ barrier is also regulated by pro-inflammatory cytokines. When mycotoxins are absorbed into the gut, inflammatory cytokines regulate the TJ barrier. In this study, DON up-regulated the mRNA expression of pro-inflammatory cytokines *IL-1β*

and *IL-8* in the duodenum of the weaned piglets. It may be that DON induces epithelial cells to produce excess pro-inflammatory cytokines, forming an inflammatory environment around the epithelial barrier, and then the pro-inflammatory cytokines change the junction localization and reorganize the cytoskeleton, thereby regulating TJ.

### 3.7. Expression levels of chemical barrier related genes

Specific intestinal epithelial cells, called goblet cells, are responsible for producing intestinal mucus, the main component of which is called



mucin. Goblet cells play a key role in barrier function because these specialized intestinal epithelial cells not only produce mucins, but also secrete factors that regulate epithelial renewal and healing (Graziani et al., 2019). Goblet cells are an important target of DON in the intestine. DON can inhibit the expression and secretion of mucin in porcine goblet cells by inhibiting PKR and MAPK-dependent resistin-like molecule  $\beta$  (RELM- $\beta$ ) (Pinton et al., 2015).

The impact of a DA on mRNA expression levels for genes related to the chemical barrier in the duodenum, jejunum, and ileum of weaned piglets is depicted in Fig. 4G–I. Relative to the CON, DON markedly suppressed the expression of MUC2 mRNA in the duodenum ( $P < 0.05$ ). However, DA did not significantly alter mRNA expression levels of chemical barrier-related genes in the jejunum and ileum ( $P > 0.05$ ). In this study, it was found that DON down-regulated the mRNA expression level of MUC2 in the duodenum, indicating that DON can affect the ability of goblet cells to produce mucin. Mucins form the intestinal mucus layer, participate in the physical and chemical barrier of the gut and provide a favorable habitat for the microbiome. A decrease in mucin reduces the gut's resistance to external pathogens. The DON dietary DA treatment showed that DA supplementation could alleviate the decrease of mucin mRNA expression to a certain extent and play a protective role.

### 3.8. The expression levels of immune barrier related genes

Cytokines play an important role in intestinal innate immune response. At low DON concentrations, DON promotes the production of immune factors that increase the risk or susceptibility to chronic disease (Zhang et al., 2020). DON can induce significantly increases in serum INF- $\gamma$ , IL-2, IL-4 and IL-6 levels. As shown in Table 2, compared with the CON group, DON significantly increased the serum concentrations of IL-6, IL-8, IL-1 $\beta$ , TNF- $\alpha$ , INF- $\gamma$  ( $P < 0.05$ ). Compared with the DON group, DA significantly decreased the serum concentrations of IL-6, IL-8, IL-1 $\beta$ , TNF- $\alpha$ , INF- $\gamma$  ( $P < 0.05$ ).

DON can induce the secretion of IgM, IgA, IgE and IgG in animals. Low doses of DON can up-regulate the expression of cytokines and inflammatory genes while stimulating the immune system, while high doses of DON can cause leukocyte apoptosis and immunosuppression. Previous studies have shown that no significant changes in serum immunoglobulin IgG and IgM concentrations were observed, when pigs were simultaneously challenged with 150  $\mu$ g/kg aflatoxins and 1.1 mg/kg DON, although there was a tendency for increase immunoglobulin levels after 42 days (Weaver et al., 2013). In another study, IgA was elevated after a DON challenge (Drochner et al., 2004), but other studies have failed to show a link between DON exposure and serum IgA levels. Whether DON stimulates serum IgA secretion is uncertain, as many studies have shown no relationship between DON exposure and IgA. One study where weaned piglets were fed a diet containing 1.2 mg/kg DON for 4 weeks, found that there was no change in IgA, IgG and IgM (Accensi et al., 2006). Similarly, in another study, weaned piglets fed a diet containing 8 mg/kg DON for 4 weeks, showed no change in IgA and only increased levels of IgM and IgG (Reddy et al., 2018). The above studies

suggest that DON contamination does not affect immunoglobulin levels, possibly because there is no change in the immune system's antibody response. This study assessed immunoglobulin production, and unlike previous studies, and found that DON did not cause changes in immunoglobulin levels. These differences in results may be due to differences in animal sex, feed composition, the state of the animals themselves, and feeding methods.

Another study showed that serum levels of IL-2, IL-1 $\beta$ , IL-6, TNF- $\alpha$  and INF- $\gamma$  were significantly increased in weaned piglets fed a diet containing 4 mg/kg DON (Zha et al., 2020). These results herein are consistent with above results, namely, DON could increase the levels of serum IL-6, IL-8, IL-1 $\beta$ , TNF- $\alpha$  and INF- $\gamma$  of weaned piglets. The reason for the change of cytokines in serum may be intestinal inflammation caused by the DON challenge in weaned piglets. DON up-regulated the gene expression of intestinal IL-8, TNF- $\alpha$ , INF- $\gamma$  and other specific cytokines. Inflammatory gene expression of TNF- $\alpha$ , IL-1 $\beta$ , IL-6, IL-10 and INF- $\gamma$  were up-regulated in the ileum and jejunum of weaned piglets fed 3 mg/kg for 5 weeks (Bracarense et al., 2012). After low dose (0.9 mg/kg) short-term (10 d) DON exposure, mRNA expression of IL-1 $\beta$  and IL-10 in the intestines of growing pigs were up-regulated (Alizadeh et al., 2015). The results of this experiment show that DON up-regulated the mRNA expression of pro-inflammatory cytokine IL-8 in duodenal and jejunal tissues of weaned piglets. The up-regulation of IL-8 mRNA expression may indicate that DON has toxic effects on the lining of the duodenal and jejunal tissue, and then causes an acute inflammatory response.

The impact of a DA on mRNA expression levels of genes associated with the immune barrier in the duodenum, jejunum, and ileum of weaned piglets is depicted in Fig. 4D–F. Compared to the control group (CON), DON significantly elevated the mRNA expression levels of IL-8, IL-1 $\beta$ , and TNF- $\alpha$  in the duodenum, and IL-8 in the jejunum ( $P < 0.05$ ). Conversely, DA significantly reduced mRNA expression levels of IL-8, IL-1 $\beta$ , and TNF- $\alpha$  in the duodenum, as well as IL-8 in the jejunum compared to the DON group ( $P < 0.05$ ). Pro-inflammatory cytokines have been shown to damage epithelial barrier function of the gut. Cytokine regulation of the TJ barrier also occurs in pathological conditions such as inflammatory bowel disease. DON can promote the production of pro-inflammatory cytokines in epithelial cells, thus leading to a pro-inflammatory environment of the epithelial barrier, and inflammatory cytokines may change the junction localization and cytoskeletal recombination, thereby regulating the cell barrier function (Moon et al., 2007). Studies have found a link between IL-8 and high intestinal permeability, and hypothesized that MAPK signaling molecules play a role in the expression of pro-inflammatory cytokines, for example, activation of the P38 MAPK pathway promotes the production of IL-6 and IL-8 in Caco-2 cells and the expression of IL-6 genes *in vivo* (Ling et al., 2016). The above studies suggest a link between MAPK activation and impairment of intestinal barrier function, possibly mediated and linked by pro-inflammatory cytokines.

Injections of trace minerals (selenium, copper, zinc, and manganese) have been found to reduce inflammation and oxidative stress during

**Table 2**  
The serum immune-related indicators on the four dietary treatments.

Items	Treatment				SEM	P-value
	CON	DA	DON	DON+DA		
IgA, $\mu$ g/mL	509.88	516.37	538.55	533.65	14.942	0.489
IgG, mg/mL	16.04	15.81	16.30	16.60	0.438	0.623
IL-6, ng/L	590.69 <sup>b</sup>	596.13 <sup>b</sup>	695.44 <sup>a</sup>	625.34 <sup>b</sup>	19.719	<0.01
IL-8, ng/L	421.93 <sup>b</sup>	416.95 <sup>b</sup>	482.79 <sup>a</sup>	419.60 <sup>b</sup>	14.931	0.014
IL-1 $\beta$ , ng/L	20.60 <sup>b</sup>	20.76 <sup>b</sup>	28.86 <sup>a</sup>	23.49 <sup>ab</sup>	1.879	0.018
TNF- $\alpha$ , pg/mL	256.29 <sup>c</sup>	251.09 <sup>c</sup>	338.44 <sup>a</sup>	285.40 <sup>b</sup>	7.308	<0.01
INF- $\gamma$ , pg/mL	1046.67 <sup>b</sup>	1074.72 <sup>b</sup>	1686.25 <sup>a</sup>	1325.42 <sup>b</sup>	105.616	<0.01

Control group (CON), weaned piglets fed with a basal diet; DA group (DA), weaned piglets fed with a basal diet+0.2 %DA; DON group (DON), weaned piglets fed with a basal diet containing 3.55 mg/kg DON; DON+DA group (DON+DA), weaned piglets fed with a basal diet containing 3.55 mg/kg DON + 0.2 % DA. Data are mean  $\pm$  SE (n = 6). <sup>a, b</sup> Different letters in the same row indicate significant differences ( $p < 0.05$ )

aflatoxin infection in lactating prolific Holstein cows, and trace minerals isolate intestinal absorption of DON by reducing ion exchange and limiting bioavailability (Pate and Cardoso, 2018). There are many enzymes in the body that require trace minerals to participate in the synthesis, for example, superoxide dismutase (SOD) is a Zn, Mn and Cu-dependent enzyme.

### 3.9. Effects of DON and DA on cecal microbiota composition

The gut is colonized by a rich microbial ecological community, and

the gut is a storage room for microorganisms, with more than  $10^{12}$  microorganisms per milliliter of feces. The appropriate composition of the intestinal microbiota and the quantitative and qualitative stability of this ecosystem are important factors in ensuring animal health. Intestinal microbiota dysregulation can induce irritable behavior, resulting in slower growth by reducing feed intake. Previous studies have shown a close relationship between intestinal microbiota dysregulation and DON, with the intestinal microbiota being a key target for DON. DON exposure may induce intestinal disease by remodeling the intestinal microbial structure, disrupting the diversity and stability of intestinal

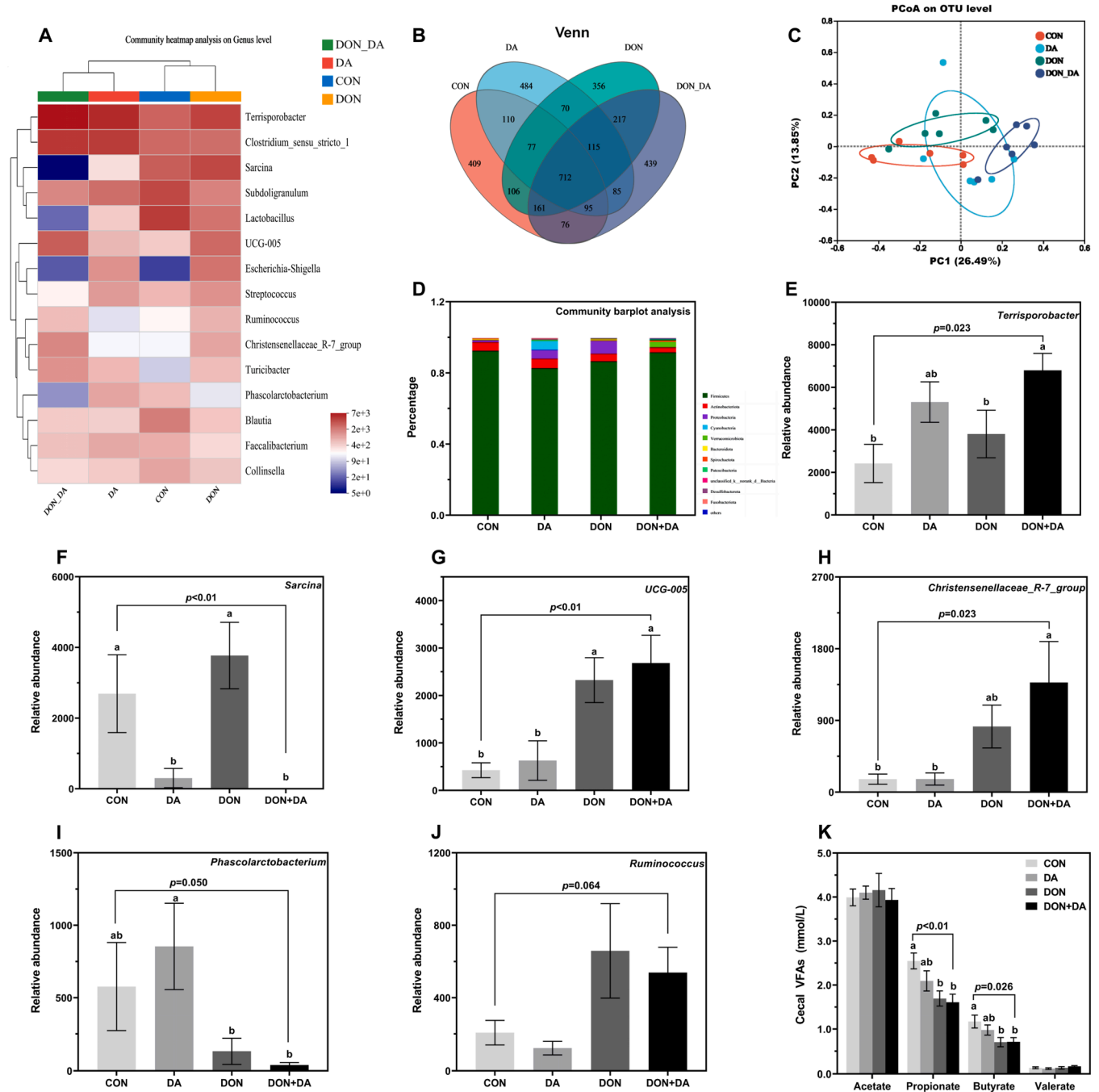


**Fig. 5.** Effects of DON and DA on the intestinal microbial composition in cecum of weaned piglets. (A) Heat map of Microbiota composition in the cecal digesta at the genus level, (B) Venn diagram was generated to compare operational taxonomic units (OTUs) between different groups, (C) PCoA cluster analysis, (D) The relative abundances of cecal bacterial at the phylum level, (E-J) Relative abundance of cecal *Terrisporobacter*, *Sarcina*, *UCG-005*, *Christensenellaceae\_R-7\_group*, *Phascolarctobacterium* and *Ruminococcus* in each group and (K) Effects of DA on the concentration of volatile fatty acid in the cecum of weaned piglets. Data are mean  $\pm$  SE ( $n = 6$ ). Data labelled with different low-case letters are statistically different at  $p < 0.05$ .

microbial community. DON-mediated intestinal microbiota dysregulation can lead to malnutrition and decreased growth performance in weaned piglets (Wang et al., 2019). PCoA results showed the separation of cecal samples between the DON group and DON + DA group. Therefore, the addition of DA to DON treated feed can affect the cecal microbiota of piglets.

Therefore, we performed sequencing of cecal microorganisms and OUT clustering. After size screening, quality control and chimera removal, 675,456 valid sequences were obtained, with an average of 409 sequences per cecal digesta sample. At the 0.03 % distance level (97 % identity), 3512 OTUs were detected in cecum samples (Fig. 5B), and 409, 484, 356 and 439 unique OUTs were detected in cecum samples of weaned piglets in the CON, DA, DON and DON + DA groups, respectively (Fig. 5A). PCoA was used to distinguish the microbiota composition of different populations according to evolutionary distance. It was found through PCoA analysis that the intestinal microbiota of weaned piglets in the DON and DON + DA groups had significant structural changes compared with that in the CON group (Fig. 5C). Firmicutes, Actinomycetes, Proteobacteria and Cyanobacteria were the four main bacterial phyla in the cecal chyme, accounting for more than 98 % of the total bacterial community in the cecum. DON and DA had no significant effect on the four main phyla (Fig. 5D;  $P > 0.05$ ). DON significantly decreased the relative abundance of *Phascolarctobacterium* (Fig. 5I;  $P < 0.05$ ), significantly increased the relative abundance of *Terrisporobacter*, *UCG-005* and *Christensenellaceae\_R-7\_group* (Fig. 5E–H;  $P < 0.05$ ). In addition, DON tended to increase the relative abundance of *Ruminococcus* (Fig. 5J;  $0.05 \leq P < 0.1$ ). Compared with the DON group, DA significantly decreased the relative abundance of *Sarcina* (Fig. 5F;  $P < 0.05$ ).

DON and DA had no significant effect on the composition and distribution of intestinal microbiota at phyla level in weaned piglets. On the genus level, DON significantly decreased the relative abundance of *Phascolarctobacterium* and significantly increased the relative abundance of *Terrisporobacter*, *Sarcina*, *UCG-005*, *Christensenellaceae\_R-7\_group*. The *Terrisporobacter* is a Gram-positive, spore-forming anaerobic bacterium once classified as *Clostridium* (Pahalagedara et al., 2023). They have been shown to ferment glucose and cellulose and are fiber-degrading bacteria at all stages of growth (Liu and Fan, 2022). The mechanism by which *Phascolarctobacterium* is regulated within the intestinal microbiota is still poorly understood, but it is certainly a beneficial microbe. *Phascolarctobacterium* contains glycoside hydrolase which is related to host-glycan degradation, which consumes succinic acid and host glycan. The increased abundance of *Phascolarctobacterium* can also consume succinate more efficiently in the intestinal, which limits the growth of *Clostridioidesdifficile* and has a certain protective effect against intestinal diseases (Nagao-Kitamoto et al., 2020). *Sarcina* are Gram-positive anaerobic bacteria that can grow in acidic environments, and an increased abundance can cause inflammation of the gut (Al Rasheed and Senseng, 2016). *Christensenellaceae\_R-7\_group* are capable of degrading carbohydrates, amino acids and carboxylic acids into acetate and butyrate (Morotomi et al., 2012). Members of *Christensenellaceae* are associated with gut health, preventing intestinal inflammation, and stimulating energy expenditure and fatty acid oxidation in the host, which helps with weight management (Guerra et al., 2022). *UCG-005* belongs to the *Oscillospirales*, and members of *UCG-005* promote fiber degradation in animals (Yang et al., 2020).

DON tended to increase the relative abundance of *Ruminococcus*. *Ruminococcus*, a member of the *Firmicutes*, are one of the most numerous families in the *Clostridiales* and is associated with maintaining intestinal health (Liang et al., 2021). Bacteria of this genus are found in the gastrointestinal tract of a variety of animals, where they play a role in the fermentation of cellulose-rich feeds and resistant starches (Morais and Mizrahi, 2019). During the natural milder process of corn, *fusarium gramineum* decomposes the endogenous starch of corn grains, which may be the reason for the increase of *ruminococcus* community richness in the intestinal tract of weaned piglets.

Feed intake, gut microbiota, and host health can be linked through signaling molecules called volatile fatty acids (VFAs). Butyrate, a major VFA species, is produced by bacteria in the gut that ferment dietary fiber. Previous studies have found that weaned piglets fed a 4 mg/kg DON diet showed decreased colonic acetate, propionate, butyrate, and total VFA concentrations (Wang et al., 2020). In the present study, as shown in Fig. 5K, compared with the CON group, DON significantly ( $P < 0.05$ ) decreased the concentrations of propionate and butyrate in the cecal contents of weaned piglets, which was consistent with the above results. DA had no significant effect on the concentration of volatile fatty acids in cecum ( $P > 0.05$ ), which may be because the effects of DON on intestinal microorganisms were long-term and could not be reversed in a short time.

#### 4. Conclusions

Incorporating 0.2 % DA resulted in a maximum degradation rate of 98.46 % for the DON standard and 49.28 % in mixed piglet feed. A minimal portion of DON dissociated in the gastrointestinal tract following detoxification, which further confirms that DA can effectively and stably degrade DON in feed. The proposed mechanism for DA-mediated DON degradation involves the oxidation of the unsaturated carbon-carbon double bonds at positions C9 and C10, as well as the epoxide groups at positions C12 and C13. This process leads to the formation of cyclopentanone and cyclohexene ether rings, effectively converting DON into di-, tri-, and tetracarboxylic acids that promote its degradation and detoxification. The incorporation of 0.2 % DA into DON-contaminated feed has demonstrated a partial mitigation of the negative effects of DON on growth performance and intestinal barrier functions. Therefore, DA presents a viable commercial strategy with significant potential for reducing DON toxicity. However, the distribution of DA and its metabolites in piglets were not examined in this study, which warrants further exploration in future research.

#### Ethics Statement

The experiment was performed following the Chinese Guidelines for Animal Welfare set by the National Institute of Animal Health and approved by the Animal Care and Use Committee of Sichuan Agricultural University.

#### CRediT authorship contribution statement

**Thomas David G:** Writing – review & editing. **Bing Wu:** Resources. **Jingping Song:** Writing – original draft. **wang xianxiang:** Project administration. **Xinyue Liu:** Writing – review & editing, Writing – original draft, Software. **Yuwei Zhang:** Resources, Data curation. **Ziyun Zhou:** Methodology. **Jian Li:** Resources, Data curation. **Fali Wu:** Resources. **Chuanmin Cheng:** Resources. **Caimei Wu:** Writing – original draft, Resources, Data curation. **Xiang Pu:** Software. **Xinru Yan:** Resources.

#### Declaration of Competing Interest

The authors declare that they have no known competing financial interests or personal relationships that could have appeared to influence the work reported in this paper.

#### Acknowledgments

This work was supported by Sichuan Science and Technology Program (No.2021ZDZX0011), “Shuangzhi plan” of Sichuan Agricultural University and the 111 project (D17015). The graphical abstract was designed by Biorender.

## Appendix A. Supporting information

Supplementary data associated with this article can be found in the online version at [doi:10.1016/j.ecoenv.2024.117246](https://doi.org/10.1016/j.ecoenv.2024.117246).

## Data Availability

Data will be made available on request.

## References

- Abasi, N., Faraji, A.R., Davood, A., 2023. Adsorptive removal of aflatoxin B1 from water and edible oil by dopamine-grafted biomass chitosan-iron-cobalt spinel oxide nanocomposite: mechanism, kinetics, equilibrium, thermodynamics, and oil quality. *RSC Adv.* 13 (49), 34739–34754. <https://doi.org/10.1039/d3ra06495f>.
- Accensi, F., Pinton, P., Callu, P., Abella-Bourges, N., Guelfi, J.F., Grosjean, F., et al., 2006. Ingestion of low doses of deoxynivalenol does not affect hematological, biochemical, or immune responses of piglets. *J. Anim. Sci.* 84, 1935–1942. <https://doi.org/10.2527/jas.2005-355>.
- Al Rasheed, M.R., Senseng, C.G., 2016. *Sarcina ventriculi*: review of the literature. *Arch. Pathol. Lab Med* 140, 1441–1445. <https://doi.org/10.1016/j.ijid.2021.11.027>.
- Alizadeh, A., Braber, S., Akbari, P., Garssen, J., Fink-Gremmels, J., 2015. Deoxynivalenol impairs weight gain and affects markers of gut health after low-dose, short-term exposure of growing pigs. *Toxins* 7, 2071–2095. <https://doi.org/10.3390/toxins7062071>.
- Anater, A., Manyes, L., Meca, G., Ferrer, E., Luciano, F.B., Pimpão, C.T., et al., 2016. Mycotoxins and their consequences in aquaculture: a review. *Aquaculture* 451, 1–10. <https://doi.org/10.1016/j.aquaculture.2015.08.022>.
- Andretta, I., Kipper, M., Lehnen, C.R., Hauschild, L., Vale, M.M., Lovatto, P.A., 2012. Meta-analytical study of productive and nutritional interactions of mycotoxins in growing pigs. *Animal* 6, 1476–1482. <https://doi.org/10.1017/s1751731111002278>.
- Avantaggiato, G., Havenaar, R., Visconti, A., 2004. Evaluation of the intestinal absorption of deoxynivalenol and nivalenol by an in vitro gastrointestinal model, and the binding efficacy of activated carbon and other adsorbent materials. *Food Chem. Toxicol.* 42, 817–824. <https://doi.org/10.1016/j.fct.2004.01.004>.
- Bracarense, A.P., Luciola, J., Grenier, B., Drociunas Pacheco, G., Moll, W.D., Schatzmayr, G., et al., 2012. Chronic ingestion of deoxynivalenol and fumonisin, alone or in interaction, induces morphological and immunological changes in the intestine of piglets. *Br. J. Nutr.* 107, 1776–1786. <https://doi.org/10.1017/s0007114511004946>.
- Cheng, L., Jiang, T., Zhang, J., 2021. Photoelectrocatalytic degradation of deoxynivalenol on CuO-Cu(2O)/WO(3) ternary film: mechanism and reaction pathways. *Sci. Total Environ.* 776, 145840. <https://doi.org/10.1016/j.scitotenv.2021.145840>.
- Council USNR, 2012. *Nutrient rEquirements of Swine, 11th ed.* National Academy Press, Washington, DC.
- Dersjant-Li, Y., Verstegen, M.W.A., Gerrits, W.J.J., 2007. The impact of low concentrations of aflatoxin, deoxynivalenol or fumonisin in diets on growing pigs and poultry. *Nutr. Res Rev.* 16, 223–239. <https://doi.org/10.1079/nrr200368>.
- Drochner, W., Schollenberger, M., Piepho, H.P., Gotz, S., Lauber, U., Tafaj, M., et al., 2004. Serum IgA-promoting effects induced by feed loads containing isolated deoxynivalenol (DON) in growing piglets. *J. Toxicol. Environ. Health A* 67, 1051–1067. <https://doi.org/10.1080/15287390490447313>.
- Garai, E., Risa, A., Varga, E., Cserhati, M., Kriszt, B., Urbanyi, B., et al., 2021. Evaluation of the multimycotoxin-degrading efficiency of *Rhodococcus erythropolis* N11 strain with the three-step zebrafish microinjection method. *Int. J. Mol. Sci.* 22, 724. <https://doi.org/10.3390/ijms22020724>.
- Graziani, F., Pinton, P., Olleik, H., Pujol, A., Nicoletti, C., Sicre, M., et al., 2019. Deoxynivalenol inhibits the expression of trefoil factors (TFF) by intestinal human and porcine goblet cells. *Arch. Toxicol.* 93, 1039–1049. <https://doi.org/10.1007/s00204-019-02425-6>.
- Guerra, V., Tiago, I., Aires, A., Coelho, C., Nunes, J., Martins, L.O., et al., 2022. The gastrointestinal microbiome of browsing goats (*Capra hircus*). *PLoS One* 17, e0276262. <https://doi.org/10.1371/journal.pone.0276262>.
- Ji, C., Fan, Y., Zhao, L., 2016. Review on biological degradation of mycotoxins. *Anim. Nutr.* 2, 127–133. <https://doi.org/10.1371/journal.pone.0276262>.
- Lafleur Larivière, E., Zhu, C., Zettell, S., Patterson, R., Karrow, N.A., Huber, L.A., 2021. The effect of deoxynivalenol-contaminated corn and an immune-modulating feed additive on growth performance and immune response of nursery pigs fed corn- and soybean meal-based diets. *Transl. Anim. Sci.* 5, txab141. <https://doi.org/10.1093/tas/txab141>.
- Liang, J., Kou, S., Chen, C., Raza, S.H.A., Wang, S., Ma, X., et al., 2021. Effects of *Clostridium butyricum* on growth performance, metabonomics and intestinal microbial differences of weaned piglets. *BMC Microbiol* 21, 85. <https://doi.org/10.1186/s12866-021-02143-z>.
- Ling, K.H., Wan, M.L., El-Nezami, H., Wang, M., 2016. Protective capacity of resveratrol, a natural polyphenolic compound, against deoxynivalenol-induced intestinal barrier dysfunction and bacterial translocation. *Chem. Res. Toxicol.* 29, 823–833. <https://doi.org/10.1021/acs.chemrestox.6b00001>.
- Liu, S., Fan, Z., 2022. Effects of dietary protein restriction on colonic microbiota of finishing pigs. *Anim. Basel* 13, 9. <https://doi.org/10.3390/ani13010009>.
- Liu, T., Xiao, S., Li, N., Chen, J., Zhou, X., Qian, Y., et al., 2023a. Water decontamination via nonradical process by nanoconfined Fenton-like catalysts. *Nat. Commun.* 14. <https://doi.org/10.1038/s41467-023-38677-1>.
- Moon, Y., Yang, H., Lee, S.H., 2007. Modulation of early growth response gene 1 and interleukin-8 expression by ribotoxin deoxynivalenol (vomitoxin) via ERK1/2 in human epithelial intestine 407 cells. *Biochem. Biophys. Res. Commun.* 362, 256–262. <https://doi.org/10.1016/j.bbrc.2007.07.168>.
- Moras, S., Mizrahi, I., 2019. The road not taken: the rumen microbiome, functional groups, and community states. *Trends Microbiol* 27, 538–549. <https://doi.org/10.1016/j.tim.2018.12.011>.
- Morotomi, M., Nagai, F., Watanabe, Y., 2012. Description of *Christensenella minuta* gen. nov., sp. nov., isolated from human faeces, which forms a distinct branch in the order Clostridiales, and proposal of Christensenellaceae fam. nov. *Int. J. Syst. Evol. Microbiol.* 62, 144–149. <https://doi.org/10.1099/ijs.0.026989-0>.
- Nagao-Kitamoto, H., Leslie, J.L., Kitamoto, S., Jin, C., Thomsson, K.A., Gilliland, M.G., 3rd, et al., 2020. Interleukin-22-mediated host glycosylation prevents Clostridioides difficile infection by modulating the metabolic activity of the gut microbiota. *Nat. Med.* 26, 608–617. <https://doi.org/10.1038/s41591-020-0764-0>.
- Pahalagedara, A., Flint, S., Palmer, J., Brightwell, G., Luo, X., Li, L., et al., 2023. Non-targeted metabolomic profiling identifies metabolites with potential antimicrobial activity from an anaerobic bacterium closely related to *Terrisporobacter* species. *Metabolites* 13, 252. <https://doi.org/10.3390/metabo13020252>.
- Palanisamy, V., Pc, S., Pineda, L., Han, Y., 2023. Effect of supplementing hydroxy trace minerals (Cu, Zn, and Mn) on egg quality and performance of laying hens under tropical conditions. *Anim. Biosci.* 36, 1709–1717. <https://doi.org/10.5713/ab.22.0416>.
- Pate, R.T., Cardoso, F.C., 2018. Injectable trace minerals (selenium, copper, zinc, and manganese) alleviate inflammation and oxidative stress during an aflatoxin challenge in lactating multiparous Holstein cows. *J. Dairy Sci.* 101 (9), 8532–8543. <https://doi.org/10.3168/jds.2018.14447>.
- Peng, H., Xiong, W., Yang, Z., Tong, J., Jia, M., Xiang, Y., et al., 2023a. Fe3O4-supported N-doped carbon channels in wood carbon form etching and carbonization: boosting performance for persulfate activating. *Chem. Eng. J.* 457, 141317. <https://doi.org/10.1016/j.cej.2023.141317>.
- Peng, H.H., Xiong, W.P., Yang, Z.H., Tong, J., Jia, M.Y., Xiang, Y.P., et al., 2023b. Fe3O4-supported N-doped carbon channels in wood carbon form etching and carbonization: boosting performance for persulfate activating. *Chem. Eng. J.* 457. <https://doi.org/10.1016/j.cej.2023.141317>.
- Pestka, J.J., Smolinski, A.T., 2005. Deoxynivalenol: toxicology and potential effects on humans. *J. Toxicol. Environ. Health B* 8, 39–69. <https://doi.org/10.1080/10937400590889458>.
- Pinton, P., Graziani, F., Pujol, A., Nicoletti, C., Paris, O., Ernouf, P., et al., 2015. Deoxynivalenol inhibits the expression by goblet cells of intestinal mucins through a PKR and MAP kinase dependent repression of the resistin-like molecule beta. *Mol. Nutr. Food Res.* 59, 1076–1087. <https://doi.org/10.1002/mnfr.201500005>.
- Ragab, W.S.M., Drusch, S., Schnieder, F., Beyer, M., 2009. Fate of deoxynivalenol in contaminated wheat grain during preparation of Egyptian 'balila. *Int. J. Food Sci. Nutr.* 58, 169–177. <https://doi.org/10.1080/09637480601040997>.
- Reddy, K.E., Song, J., Lee, H.J., Kim, M., Kim, D.W., Jung, H.J., et al., 2018. Effects of high levels of deoxynivalenol and zearalenone on growth performance, and hematological and immunological parameters in pigs. *Toxins* 10, 114. <https://doi.org/10.3390/toxins10030114>.
- Schwartz, H.E., Hametner, C., Slavik, V., Greitbauer, O., Bichl, G., Kunz-Vekiru, E., et al., 2013. Characterization of three deoxynivalenol sulfonates formed by reaction of deoxynivalenol with sulfur reagents. *J. Agric. Food Chem.* 61, 8941–8948. <https://doi.org/10.1021/jf403438b>.
- Su, X., Wang, S., Wang, X., Ji, W., Zhang, H., Tu, T., Hakulinen, N., Luo, H., Yao, Bin, Zhang, W., Huang, H., 2024. Targeting deoxynivalenol for degradation by a chimeric manganese peroxidase/glutathione system. *Ecotoxicol. Environ. Saf.* 273, 116130. <https://doi.org/10.1016/j.ecoenv>.
- Tang, M., Yuan, D., Liao, P., 2021. Berberine improves intestinal barrier function and reduces inflammation, immunosuppression, and oxidative stress by regulating the NF-kappaB/MAPK signaling pathway in deoxynivalenol-challenged piglets. *Environ. Pollut.* 289, 117865. <https://doi.org/10.1016/j.envpol.2021.117865>.
- Verdile, N., Mirmahmoudi, R., Brevini, T.A.L., Gandolfi, F., 2019. Evolution of pig intestinal stem cells from birth to weaning. *Animal* 13, 2830–2839. <https://doi.org/10.1017/s1751731119001319>.
- Vila-Donat, P., Marin, S., Sanchis, V., Ramos, A.J., 2018. A review of the mycotoxin adsorbing agents, with an emphasis on their multi-binding capacity, for animal feed decontamination. *Food Chem. Toxicol.* 114, 246–259. <https://doi.org/10.1016/j.fct.2018.02.044>.
- Wang, Y.H., Sun, Y.L., Wang, R.Y., Gao, M.C., Xin, Y.J., Zhang, G.S., et al., 2023. Activation of peroxymonosulfate with cobalt embedded in layered 8-MnO2 for degradation of dimethyl phthalate: Mechanisms, degradation pathway, and DFT calculation. *J. Hazard. Mater.* 451. <https://doi.org/10.1016/j.jhazmat.2023.130901>.
- Wang, S., Yang, J., Zhang, B., Zhang, L., Wu, K., Yang, A., et al., 2019. Potential link between gut microbiota and deoxynivalenol-induced feed refusal in weaned piglets. *J. Agric. Food Chem.* 67, 4976–4986. <https://doi.org/10.1021/acs.jafc.9b01037>.
- Wang, S., Zhang, C., Yang, J., Wang, X., Wu, K., Zhang, B., et al., 2020. Sodium butyrate protects the intestinal barrier by modulating intestinal host defense peptide expression and gut microbiota after a challenge with deoxynivalenol in weaned piglets. *J. Agric. Food Chem.* 68, 4515–4527. <https://doi.org/10.1021/acs.jafc.0c00791>.
- Weaver, A.C., See, M.T., Hansen, J.A., Kim, Y.B., De Souza, A.L., Middleton, T.F., et al., 2013. The use of feed additives to reduce the effects of aflatoxin and deoxynivalenol



- on pig growth, organ health and immune status during chronic exposure. *Toxins* 5, 1261–1281. <https://doi.org/10.3390/toxins5071261>.
- Yang, C., Tsedan, G., Liu, Y., Hou, F., 2020. Shrub coverage alters the rumen bacterial community of yaks (*Bos grunniens*) grazing in alpine meadows. *J. Anim. Sci. Technol.* 62, 504–520. <https://doi.org/10.5187/jast.2020.62.4.504>.
- Zha, A., Cui, Z., Qi, M., Liao, S., Yin, J., Tan, B., et al., 2020. Baicalin-copper complex modulates gut microbiota, inflammatory responses, and hormone secretion in DON-challenged piglets. *Animals* 10, 1535. <https://doi.org/10.3390/ani10091535>.
- Zhang, L., Ma, R., Zhu, M.X., Zhang, N.Y., Liu, X.L., Wang, Y.W., et al., 2020. Effect of deoxynivalenol on the porcine acquired immune response and potential remediation by a novel modified HSCAS adsorbent. *Food Chem. Toxicol.* 138, 111187. <https://doi.org/10.1016/j.fct.2020.111187>.